THE NONLINEARITY OF REGULATION IN BIOLOGICAL NETWORKS

Santosh Manicka[*] Tufts University
Kathleen Johnson* University of Kentucky
Michael Levin Tufts University
David Murrugarra[†] University of Kentucky

March 29, 2023

ABSTRACT

The extent to which the components of a biological system are (non)linearly regulated determines how amenable they are to therapy and control. To better understand this property termed 'regulatory nonlinearity', we analyzed a suite of 137 published Boolean network models, containing a variety of complex nonlinear regulatory interactions, using a probabilistic generalization of Boolean logic that George Boole himself had proposed. Leveraging the continuous-nature of this formulation, we used Taylor decomposition to approximate the models with various levels of regulatory nonlinearity. A comparison of the resulting series of approximations of the biological models with appropriate random ensembles revealed that biological regulation tends to be less nonlinear than expected, meaning that higher-order interactions among the regulatory inputs tend to be less pronounced. A further categorical analysis of the biological models revealed that the regulatory nonlinearity of cancer and disease networks could not only be sometimes higher than expected but also relatively more variable. We show that this variation is caused by differences in the apportioning of information among the various orders of regulatory nonlinearity. Our results suggest that there may have been a weak but discernible selection pressure for biological systems to evolve linear regulation on average, but for certain systems such as cancer, on the other hand, to also evolve more nonlinear rules.

Keywords Nonlinearity · Biological networks · Boolean decomposition

1 Introduction

How nonlinear is the regulation of the components of biological networks? That is, to what extent do the biochemical components of these networks non-independently interact (Fig 1) in influencing downstream processes and network behavior. Research on the 'nonlinearity' front has hitherto focused on its various manifestations in the dynamics of biological systems, such as chaos, bifurcation, multistability, synchronization, patterning, dissipation, etc.[1], but a characterization of *regulatory* nonlinearity among the components of the underlying systems that give rise to those phenomena is lacking. A more complete understanding of biological regulatory nonlinearity would not only yield insights into their design principles [2] but also have theoretical implications ranging from canalization to control [3, 4] and practical implications for biomedical therapy, synthetic biology, etc. [1, 5]. A good example of this concerns the mapping between molecular or genetic information and the resulting system-level anatomical structure and function of an organism. Advances in regenerative medicine and synthetic morphology require rational control of physiological and anatomical outcomes [6], but progress in genetics and molecular biology produce methods and knowledge targeting the lowest-level cellular hardware. There is no one-to-one mapping from genetic information to tissue- and organ-level structure; similarly, ion channels open and close post-translationally, driving physiological dynamics that are not readily inferred from proteomic or transcriptomic data. System-level properties in biology are often highly emergent, with gene-regulatory or bioelectric circuit dynamics connecting initial state information and transition rules to large-scale

[*] Author contributions: S.M. and D.M. conceived the study; S.M. and K.J. designed code; K.J. performed research and simulations; S.M., K.J., and D.M. analyzed data; M.L. helped bridge the theory to biology. All authors helped in the writing of the manuscript. All authors approved the final version of the manuscript.
The Authors declare no Competing Financial or Non-Financial Interests.
*S.M. contributed equally to this work with K.J.
†To whom correspondence should be addressed. E-mail: murrugarra@uky.edu

structure and function. Thus, the difficult inverse problem [7] of inferring outcomes and desirable interventions across scales of biology illustrates some of the fundamental questions about the directness or nonlinearity of encodings of information, as well as the importance of this question for practical advances in biomedicine and bioengineering that exploit the plasticity and robustness of cellular collectives. Many deep questions remain about the potential limitations and best strategies to bridge scales for prediction and control in developmental, evolutionary, and cell biology. To that end, we introduce here a formal characterization of the nonlinearity of models of biological regulatory networks, such as those often used to describe relationships between regulatory genes. Specifically, we consider a class of discrete models of biological regulatory systems called "Boolean models" that are known for their relative simplicity and tractability compared to continuous ordinary differential equation-based (ODE) models [8].

A Boolean network is a discrete network model characterized by the following features. Each node in a Boolean network can only be in one of two states, ON or OFF, which represents the expression or activity of that node. The state of a node depends on the states of other input nodes which are represented as a Boolean rule of these input nodes. Many of the available Boolean network models were created via literature search of the regulatory mechanisms and subsequently validated via experiments [9]. Some of the publicly available models were generated via network inference methods from time course data [3].

Previous studies have found that certain characteristic features of the biological Boolean models, such as the mean in-degree, output bias, sensitivity and canalization, tend to assume an optimal range of values that support optimal function [10, 11]. Here we study a new but generic feature of complex systems termed "regulatory nonlinearity" that we broadly define as the degree to which the inputs to the components of a complex interact. To characterize the regulatory nonlinearity of Boolean networks we formalize an approach to generalizing Boolean logic by casting it as a form of probability, which was originally proposed by George Boole himself [12]. We leverage the continuous nature of these polynomials to decompose a Boolean function using Taylor-series and reveal the distinct layers of its regulatory nonlinearity (Fig 2). Various other methods, both discrete and continuous, of decomposing Boolean functions exist, such as Reed-Muller, Walsh spectrum, Fourier, discrete Taylor and fuzzy logic [13, 14, 15, 16]. Our continuous Taylor decomposition method is distinct in that it offers a clear and systematic way to characterize nonlinearity.

Is the regulatory nonlinearity of biological systems special? To that end we specifically ask: 1) how well could biological Boolean models be approximated, that is, faithfully represented with only partial information containing lower levels of nonlinearity relative to that of the original?; 2) is there an optimal level of regulatory nonlinearity, characterized by maximum approximability, that these models may have been selected for by evolution?; and 3) do different classes of biological networks show characteristically different optimal levels of regulatory nonlinearity? To answer these questions, we first approximate the biological models by systematically composing the various nonlinear layers resulting in a sequence of model-approximations with increasing levels of nonlinearity. We then estimate the accuracy of these approximations by comparing the outputs of their simulations with that of the original unapproximated model. We then construct an appropriate random ensemble for each biological model and compare their mean accuracies for fixed levels of approximation. The main idea is that a biological model that is more approximable than expected for a particular level of nonlinearity would mean that the network may have been optimized for that level nonlinearity. Finally, we classify the biological networks into various categories and compare their approximabilities to identify any category-dependent effects.

Methods

Probabilistic generalization of Boolean logic

Here we provide a continuous-variable formulation of a Boolean function by casting Boolean values as probabilities, thus transforming it into a pseudo-Boolean function [18]. Consider random variables $X_i : \{0,1\} \to [0,1]$, $i = 1, \ldots, n$, with Bernoulli distributions. That is, $p_i = Pr(X_i = 1) = 1 - Pr(X_i = 0) = 1 - q_i$, for $i = 1, \ldots, n$. Let $X = X_1 \times \cdots \times X_n$ be the product of random variables and $f : X \to \{0,1\}$ a Boolean function. Let $R_0^f = \{x \in X : f(x) = 0\}$ and $R_1^f = \{x \in X : f(x) = 1\}$. Note that X is a disjoint union of R_0^f and R_1^f. Then, $Pr(f = 1) = Pr(R_1^f) = \sum_{x \in R_1^f} Pr(x) = \sum_{x \in R_1^f} \prod_{i=1}^n \hat{p}_i$ where $\hat{p}_i = p_i$ if $x_i = 1$ and $\hat{p}_i = 1 - p_i$ if $x_i = 0$. Let $\hat{f}(p_1, \ldots, p_n) = \sum_{x \in R_1^f} \prod_{i=1}^n \hat{p}_i$. Thus, $\hat{f} : [0,1]^n \to [0,1]$ is a continuous-variable function. The following theorem shows that $\hat{f}$ is a generalization of f in the sense that $\hat{f}(x) = f(x)$ for all $x \in \{0,1\}^n$; proof is provided in SI Appendix.

Theorem 1.1. *For discrete values of $x_i \in \{0,1\}$, $i = 1, \ldots, n$, we have $\hat{f}(x_1, \ldots, x_n) = f(x_1, \ldots, x_n)$.*

Corollary 1.2. *If $p_i = 1/2$ for all $i = 1, \ldots, n$, then $\hat{f}(p_1, \ldots, p_n)$ is the output bias of f.*

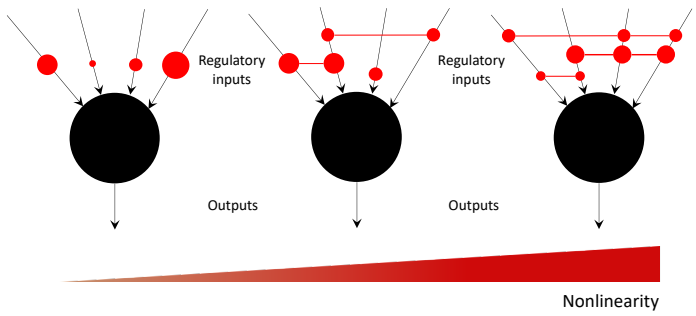

Figure 1: An illustration of the concept of regulatory nonlinearity. Each black circle represents a generic biochemical component such as a gene, transcription factor, enzyme, etc., regulated by a set of inputs (also biochemical components) and generates a generic output such as concentration level, strength, etc. Non-zero interactions among the inputs are represented by red circles connected by red lines, with the total number of possible interactions for a node with k inputs equal to $\sum_{l=1}^{k}\binom{k}{l}$. The size of the red circles and the width of the connecting lines represents the weight of the interactions. Independent inputs are represented by unconnected red circles. The degree of nonlinearity would thus be expected to increase, though not necessarily linearly, from left to right, as the numbers and the strengths of the regulatory interactions increase. One could also visualize these local interactions in a broader network-context as "hypergraphs" [17].

Example 1.3. *Consider the AND, OR, XOR, and NOT Boolean functions given in Table 1. The continuous-variable generalization of f_1, f_2, f_3, and f_4 are: $\hat{f}_1 = x_1x_2$, $\hat{f}_2 = (1-x_1)x_2 + x_1(1-x_2) + x_1x_2 = x_1 + x_2 - x_1x_2$, $\hat{f}_3 = (1-x_1)x_2 + x_1(1-x_2) = x_1 + x_2 - 2x_1x_2$, and $\hat{f}_4 = 1 - x$.*

Note that the above expressions have previously been derived via other (not probability-based) means [15, 16].

x_1	x_2	f_1	f_2	f_3
0	0	0	0	0
0	1	0	1	1
1	0	0	1	1
1	1	1	1	0

x	f_4
0	1
1	0

Table 1: Truth tables of basic Boolean functions.

Taylor Decomposition of Boolean functions

Since $\hat{f}$ is a continuous-variable function, we can calculate its Taylor expansion. And since $\hat{f}$ is a square-free polynomial, its Taylor expansion is finite and simplified (any term containing multiple derivatives of the same variable is zeroed out), as described in Proposition 1.4 using the standard multi-index notation. Let $\alpha = (\alpha_1, \ldots, \alpha_n)$ where $\alpha_i \in \{0, 1\}$. We define $\mid \alpha \mid = \alpha_1 + \cdots + \alpha_n$, $x^\alpha = x_1^{\alpha_1} x_2^{\alpha_2} \cdots x_n^{\alpha_n}$, and $\partial^\alpha f = \partial_1^{\alpha_1}\partial_2^{\alpha_2}\cdots\partial_n^{\alpha_n} f = \frac{\partial^{|\alpha|} f}{\partial_1^{\alpha_1}\partial_2^{\alpha_2}\cdots\partial_n^{\alpha_n}}$.

Proposition 1.4. *For $p \in [0,1]^n$, we have*

$$\hat{f}(x) = \hat{f}(p) + \textstyle\sum_{1<|\alpha|\leq n} \partial^\alpha \hat{f}(p)(x-p)^\alpha. \tag{1}$$

Note that $\hat{f}(p)$ in Equation 1 is the output bias of f as was seen in Corollary 1.2. A natural choice for p is $p = (1/2, \ldots, 1/2)$ as it represents an unbiased selection for each variable and it also gives the output bias of the function. Such unbiased choices are not available for the discrete case. Our continuous formulation thus offers such unique advantages over the discrete Taylor decomposition, as it's a natural generalization of the latter. The Taylor decomposition can be used to approximate a Boolean function by considering a subset of the terms. For example, a linear approximation consists of terms only up to $|\alpha| \leq 1$, a bilinear approximation up to $|\alpha| \leq 2$, etc., up until $|\alpha| \leq n$ where it ceases to be an approximation and provides an exact decomposition of $\hat{f}$. A visual illustration is provided in Figure 2. The approximation order of a Boolean *network* could therefore vary between its minimum and maximum in-degrees (number of inputs per node).

Example 1.5. *Consider the continuous generalizations of the AND, OR, XOR and NOT functions given in Example 1.3 The corresponding Taylor expansions using Equation 1 and using the derivatives shown in Table 2 with $p = (1/2, 1/2)$ are: $\hat{f}_1 = 0.25 + 0.5(x_1 - 0.5) + 0.5(x_2 - 0.5) + (x_1 - 0.5)(x_2 - 0.5)$, $\hat{f}_2 = 0.75 + 0.5(x_1 - 0.5) + 0.5(x_2 - 0.5) - (x_1 - 0.5)(x_2 - 0.5)$, $\hat{f}_3 = 0.5 - 2(x_1 - 0.5)(x_2 - 0.5)$, and $\hat{f}_4 = 0.5 - (x - 0.5) = 1 - x$.*

Derivative	f_1	f_2	f_3
∂_1	0.5	0.5	0
∂_2	0.5	0.5	0
$\partial_1\partial_2$	1	-1	-2

Derivative	f_4
∂_1	-1

Table 2: Values of partial the derivatives in the Taylor decompositions of the generalizations of basic Boolean functions.

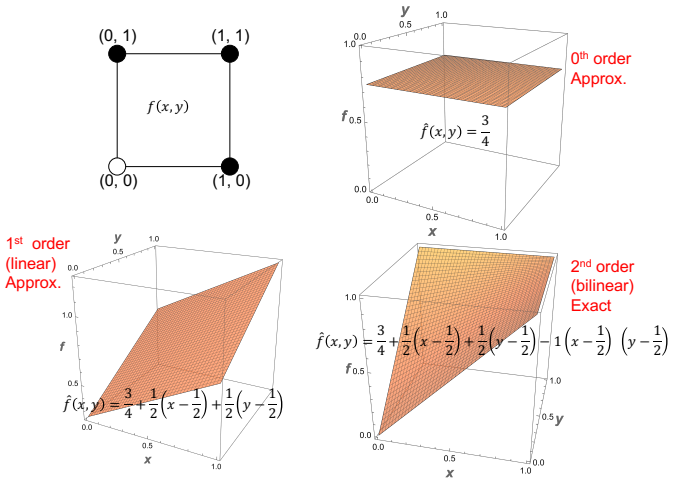

Figure 2: The various approximations of a Boolean function in increasing order of nonlinearity. The logical OR function is represented as a 2D hypercube (top left) with the coordinate values representing input combinations and the color of the circles representing the corresponding outputs (white=0, black=1) and is approximated using Taylor decomposition as the 0th order approximation (top right) showing only the first term, the mean output bias; the 1st order approximation (bottom left) including the linear terms; and finally the 2nd order exact form (bottom right) including all the terms.

Note that $\hat{f}_1(1/2, 1/2) = 0.25$, $\hat{f}_2(1/2, 1/2) = 0.75$, $\hat{f}_3(1/2, 1/2) = 0.5$, and $\hat{f}_4(1/2) = 0.5$ in the above equations are the output biases of the AND, OR, XOR, and NOT functions respectively. Also note that both the AND and OR functions contain the linear and the second order terms in their Taylor decomposition while the XOR function only contains the second order term. This difference is because both the AND and OR functions are monotone while XOR is not since it requires both inputs to be known.

Approximability of a model

We considered a suite of Boolean network models of biochemical regulation from two sources, namely the *cell collective* [9] and reference [3]. This suite consists of 137 networks with the number of nodes ranging from 5 to 321. The mean in-degree of these models ranges from 1.1818 to 4.9375 with the variances ranging between 0.1636 and 9.2941, while the mean output bias is limited to the range [0.1625,0.65625] with the variances between 0.0070 and 0.0933. For each biological model an ensemble of 100 randomized models was generated each of whose connectivity and output biases were set to be the same as the former, with only the logic rules randomized. This set, referred to as the 'constrained ensemble', facilitates benchmarking the role of regulatory nonlinearity in the biological rules. To accurately assess the difference between the biological models and the constrained ensembles, we considered a baseline set known as the 'unconstrained ensemble' relative to which those differences were computed. This ensemble preserved neither the connectivity nor the output bias but had them bootstrap-sampled from the corresponding distributions characterizing the associated biological models. Taylor decomposition was then applied to both the biological models and the random ensembles and all possible nonlinear approximations were computed by considering terms starting from the linear order accumulating up to the maximum possible nonlinear order. Both the biological models and the random ensembles were then simulated using a set of 1000 randomly chosen initial states iterated through 500 update steps for all orders of approximation; the same initial conditions were used for a given biological model and the random ensemble. The states of the variables were restricted to the interval [0,1] at every step during the simulations by simply resetting them to the nearest boundary of the interval whenever they crossed it. The mean approximation error (MAE) of each model is defined as the mean squared error between the exact Boolean states and the approximated probabilistic states at the end of the simulations; for the random ensembles a single average MAE was computed. It varies between 0.0 and 1.0. The "percentage change in MAE" (PMAE) of the biological models and the constrained ensembles is defined as the

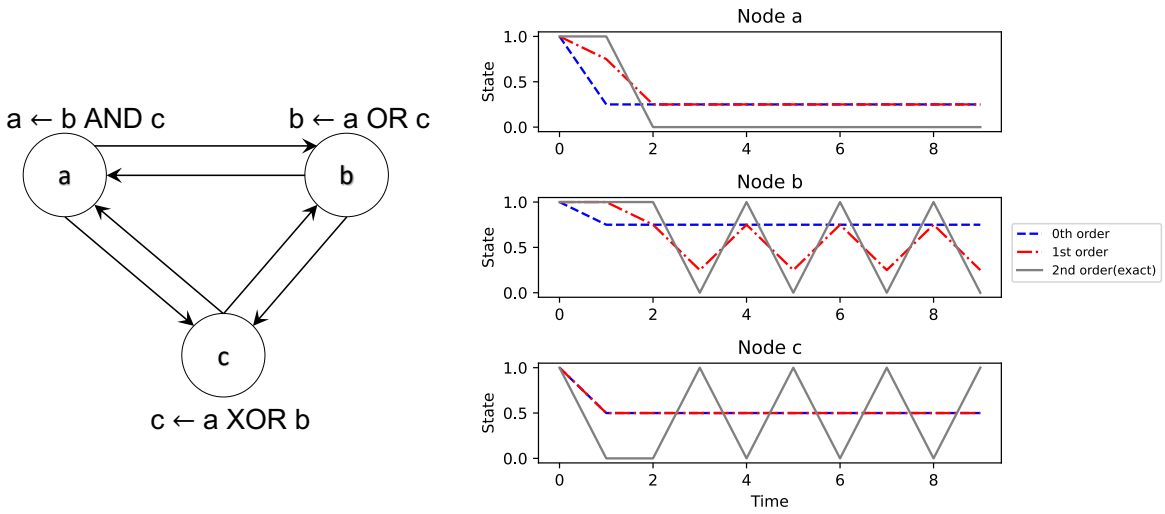

Figure 3: An illustration of the relationship between nonlinearity and approximability using a simple 3-node Boolean network. It shows that the higher the order of nonlinearity of the network the more approximable it is with respect to the exact dynamics. Left: An example 3-node network utilizing all three 2-input Boolean functions. Right: The network is simulated from a single initial state of (1,1,1). Here the dynamics of the 0th order network (blue) least matches the exact Boolean trajectory (grey), while 1st order network (red) is a slightly better match. The 2nd order network (grey) is exact since it includes all the Taylor terms up to the maximum possible order of 2 (the maximum in-degree of any node). The closer the approximated average dynamics to the exact dynamics, the lower the MAE and the higher the approximability of the former. Notice also that while for node 'a' the 0th order network is almost as good as the 1st order network, it's the opposite for node 'c' in that its 1st order approximation is as poor as the 0th order; this is because 'c' implements the XOR function whose 1st order derivatives are zero.

percentage difference between the respective MAE and the corresponding unconstrained MAE; it can vary between -100.0 and positive infinity. The "approximability" of a biological model is represented by the difference between the PMAE of the corresponding constrained ensemble and that of itself; it can vary between negative infinity and positive infinity. Hence, the more negative the PMAE is for biological models compared to that of constrained ensembles the more approximable they are deemed to be and the more unique their regulatory nonlinearity is. An illustration of how approximability is computed is provided in Figure 3.

Classification of biological models

To identify any differences among the approximabilities of different types of biological networks we sought to classify them. Since there are multiple ways to classify biological networks, we chose two classifications so that: 1) they are as orthogonal as possible to each other; and 2) each classification has an appropriate number of (neither too few nor too many) categories. Classification 1 (C1) follows the "pathway ontology" (PW) [19] where the networks are grouped into five categories (Figure 5(a)), namely biochemical ($n = 13$), signaling ($n = 22$), disease ($n = 55$), metabolic ($n = 14$) and regulatory ($n = 33$). According the definitions used in the PW ontology, a "signaling" network comprises mainly of extracellular signal transduction components such as growth factors, kinases, etc. A "regulatory" network, on the other hand, comprises intracellular transcriptional components such as genes, transcription factors, etc. The term "biochemical" here refers to networks that comprises a mix of signaling and regulatory components. "Metabolic" networks consist of components involved in the synthesis and conversion of biomolecules such as enzymes and lipids. Finally, "disease" networks consist of components involved in diseases such as cancer, anemia, pathogenic ailments and disorders such as cell cycle malfunction. Classification 2 was suggested by in-house expertise, where the networks are grouped into four categories (Figure 5(b)), namely metazoan ($n = 85$), cancer ($n = 24$), primitive ($n = 19$) and plants ($n = 9$). The "metazonan" category refers to multicellular organisms and "primitive" refers to unicellular organisms. A given model could naturally belong in multiple categories within a classification but is assigned a unique category for the purpose of simplicity; we chose the categories according to the emphasis laid in the abstracts of the corresponding publications. More details are provided in the SI Appendix (Table S1).

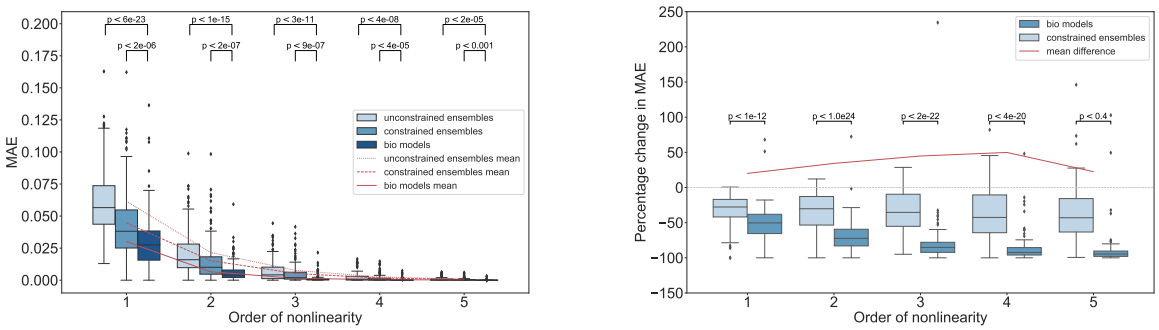

(a) (b)

Figure 4: Biological models are more approximable than expected by chance. (a) The MAE of the biological models and the associated constrained and unconstrained ensembles for approximation orders 1 to 5; MAE values for orders 6 and above are negligible and not shown. (b) Percentage change in MAE for the biological models and the associated constrained ensembles computed with respect to the MAE of the corresponding unconstrained ensembles. Every point in the distributions corresponding to the random ensembles represents the average MAE of an ensemble of 100 random networks associated with each biological model. The p-values indicate the statistical significance of the difference in mean MAEs between sets of random ensembles and the biological models for a given order of nonlinearity. Statistical analysis by Welch's unequal variances t-test.

Results and Discussion

The regulation of biological models tends to be less nonlinear than expected by chance

The MAE of biological models tends to be less than both the constrained and the unconstrained random ensembles across all approximation orders (Fig 4(a)). At the linear order, for example, the mean MAE of biological models is about 0.025, whereas the mean MAE of the constrained ensembles is twice as large at about 0.05 ($p < 10^{-6}$) and even larger for the unconstrained ensembles at about 0.07 ($p < 10^{-23}$). This ordering of MAE extends to all approximation orders (Fig 4(a)). Even though the mean MAE of even the unconstrained ensembles tends to be remarkably low (0.07 at worst), the PMAE convey a more accurate sense of approximability. For example, the MAE of the biological models and the constrained ensembles are respectively about 50% and 25% lower than the baseline expectation for the linear order (Fig 4(b)). This means that the biological models are about 25% more linearly approximable than expected by chance, an effect that amplifies with higher approximation orders going up to 50% for order 4, since the PMAE of biological models shrinks faster than the constrained ensembles (Fig 4(b)).

A possible explanation for the observed trends is that the Taylor spectrums of the biological models tend to be lopsided and more clustered at the linear ends (see Fig 6 for an example), dramatically reducing the load on the higher orders and thus resulting in a faster growth of approximability with higher orders. This effect may be less pronounced in constrained ensembles, and even less in unconstrained ensembles, as the apportioning in the corresponding Taylor spectrums may be less lopsided and more uniform in comparison. Based on these observations we hypothesize, but do not conclude, that biological systems may have been subjected to a slight but discernible selection pressure for developing less nonlinear regulatory rules. This hypothesis is further supported by the fact that the approximability systematically increases as more biological constraints are imposed as one goes from unconstrained to constrained to the biological models (Fig 4). This has implications not only for the feasibility of biomedical approaches to control emergent somatic complexity or guided self-assembly of novel forms [20], but also for models of anatomical homeostasis and evolvability: linearity implies easier control of its own complex processes by any biological system, and more efficient credit assignment during evolution.

Random models with minimal biological constraints tend to be naturally approximable

The MAE of the unconstrained random ensembles are remarkably low with values averaging around 0.07 and not exceeding 0.17 at the linear order; these values only decrease further with higher approximation orders (Fig 4(a)). These observations suggest that even random Boolean models with minimal biological constraints tend to be considerably approximable. In other words, approximability may be a natural property of random Boolean ensembles and not necessarily a special property of biological models. Furthermore, the MAE has its inflection point at order 2 (Fig

4(a)), meaning that the approximability starts saturating at that order. We hypothesize based on these observations that regulatory information beyond the bilinear order may be inconsequential with regards to the statistics of network dynamics in general.

The above hypothesis has an analogue in the realm of Boolean Ising models, where it was found that maximum entropy (MaxEnt) models with only pairwise interactions were sufficient to fit random multivariate Ising networks that are densely connected and whose state spaces satisfy certain entropy constraints, features that many biological systems share [21]. There are however important differences between our results and theirs: a) even though the Taylor expansions resemble MaxEnt expressions, the latter fit global state-space distributions, whereas our Taylor polynomials are local formulations; and b) whereas our Taylor polynomials are built on derivatives of the states, MaxEnt models are based on the raw values. Notwithstanding these potentially superficial differences, the analogous results are striking and calls for further research on whether the respective explanations are similar if not fundamentally the same. Besides, the above observations are reminiscent of the concept of model degeneracy or 'sloppiness', where several models (defined by unique sets of parameters) explain the same biological phenomenon due to redundant parameters [22]. In our case, it's not the parameters but the higher-order relationships among them that are redundant, as they contribute minimally to the MAE beyond a certain order of approximation (Fig 4(a)). Future research will determine whether there's a deep connection between the sloppiness of the parameters and the orders of relationships among them.

The approximability of a biological model depends on its class, with the cancer family displaying the most variability

Even though the nonlinearity of biological networks is less than expected on average, individual and category-dependent variations were observed. In the following, we focus on the "linear approximability" (PMAE corresponding to the linear order) of the biological models since we didn't observe any order-dependent differences among the models (Figure 4(b)); details are listed in SI Table 1. First, there are a few networks in almost every category that are more nonlinear than expected as evidenced by the negative linear approximability values (Fig 5). Second, the disease networks in C1 and the cancer networks in C2 are the ones with the most linear approximability (high positive values 75%). In other words, the cancer or disease pathways tend to be more optimized for linearity compared to the other categories. This makes sense since a more linear pathway is more amenable to control, which presumably works in favour of the agents of disease. Moreover, the disease and cancer networks also display the highest variability in their linear approximability compared to other categories ($p < 0.05$ in all comparisons for the cancer models), with the PMAE values ranging between -92% and 80%. In other words, disease and cancer models could be either relatively extremely more linear or nonlinear than expected, depending on the specific cases. Note that about 56% of the disease category comprises of non-cancer networks (31/55), which suggests that the effect is not significantly biased by cancer networks. These observations suggest that regulatory nonlinearity may offer an effective "entry point" to the agents of disease by virtue of its natural heterogeneity that they could leverage to their advantage perhaps as a means to evade treatment since there's no single level of nonlinearity to target. This heterogeneity may also have a connection to one of the hallmarks of cancer, namely genetic heterogeneity [23] where the cancerous cells within an individual display heterogeneous gene expression compared to the homogeneous expression in the healthy cells. In the case of nonlinearity, the heterogeneity manifests at the population level, raising the question of whether it may also be observed at the level of single cells within an individual. In other words, could the heterogeneity of nonlinearity be yet another hallmark of cancer?

The shape of the Taylor spectrum explains the extreme opposite characters of linear approximability of a pair of cancer models

Why are some models more linearly approximable and others less? The answer lies in the organization of the corresponding Taylor decompositions, as described above. To illustrate this in detail, we compared the Taylor decompositions of a pair of models chosen from among the most extreme outliers of linear approximability in either direction (Fig 5). Those models are respectively the following: a linear model describing the role of the protein p53 in the regulation of cell-cycle arrest in breast cancer [24] and henceforth referred to as the 'P53' model; and a nonlinear model describing the role of mutations in the regulation of metastasis in lung cancer [25] and henceforth referred to as the 'Metastasis' model. P53 has a linear approximability of about 72%, and it consists of 16 nodes with a mean in-degree of 3.8±2.4 and a mean output bias of 0.38±0.14; and, Metastasis has a linear approximability of about -79%, and it consists of 32 nodes with a mean in-degree of 4.9±2.5 and a mean output bias of 0.27±0.26. Thus, while P53 is smaller and sparser than Metastasis, its nodes exhibit more output-uncertainty compared to Metastasis. According to the mean field theory of random Boolean networks [26], the opposite characters of the mean in-degree and the output bias of these models means that their dynamical behaviors could be expected to be similar (although with the caution that the theory was originally developed for infinite-sized and homogeneously connected networks, which is not the case here). However, we know that their linear approximabilities, which is another expression of dynamical behavior, are opposites. One explanation for this discrepancy lies in the distinct apportioning of nonlinearity in their respective

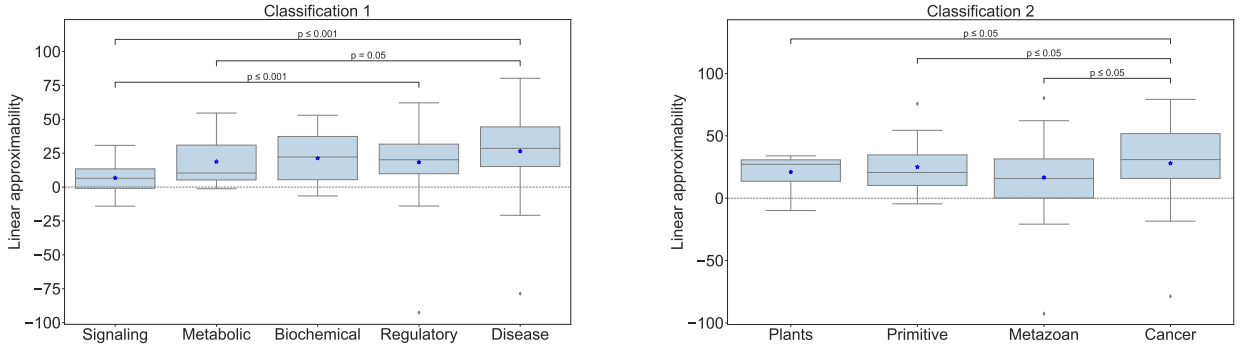

(a) (b)

Figure 5: The linear approximabilities of various categories of biological models. (a) Classification 1 (C1); (b) Classification 2 (C2). The categories in either classification are displayed in increasing order of variance. Each box represents the distribution of the linear approximabilities of the corresponding category. The p-values indicate the statistical significance of the difference in the variance between pairs of categories; only the p-values of significantly different pairs are shown. Statistical analysis by F-test of equality of variances.

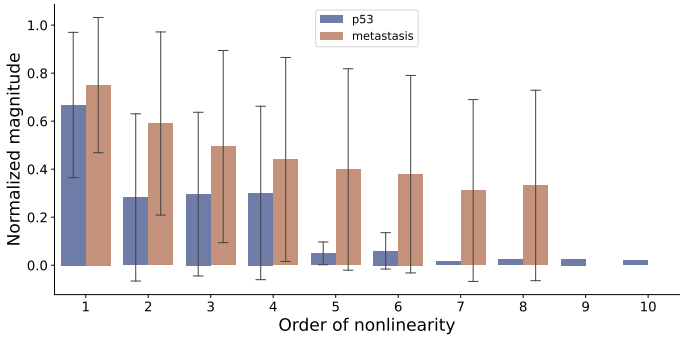

Figure 6: A comparison of the spectrums of the magnitudes of nonlinearity of the models corresponding to the two extreme cases of approximability. The bars represent the mean absolute value of all the Taylor derivatives of the corresponding order, averaged over all the nodes of the corresponding model containing those terms. The maximum orders (in-degrees) of P53 and Metastasis are respectively 10 and 8. and To compare the derivatives from different models they were normalized with respect to the maximum possible absolute value of a Taylor derivative of order $|\alpha|$ (Equation 1) of a Boolean function with output bias p, given by $(\min(p, 0.5) - \max(p - 0.5, 0))2^{|\alpha|}$ (proof provided in the SI Appendix). The error bars represent the standard deviation and not the confidence intervals of the means since they are not estimates. The errors appear large whenever the corresponding distribution of the magnitudes are bimodal with many values clustered close to 0.

Taylor decompositions (Fig 6). Specifically, while the magnitude of nonlinearity, defined as the mean absolute value of the Taylor derivatives for a given order and normalized appropriately (see text of Fig 6), tends to be clustered around the linear order for P53, they are relatively more spread out for Metastasis. Moreover, while the magnitude of the linear order for P53 is more than twice as large the next largest magnitude at lower orders the corresponding ratios for Metastasis are relatively smaller, thus explaining why P53 is more linearly approximable than Metastasis. This result is consistent with predictions based on a model of scaling of cellular control policies [27]. A more controllable (linear) network (P53) is optimal for cooperation with other cells towards collective (normal morphogenetic) goals. In contrast, a cell defecting from the collective and reverting to a more unicellular lifestyle (Metastasis) should exhibit a less predictable, controllable network due to pressures from parasites and competitors that independent unicellular organisms face. Methods for calculating controllability (e.g., linearity) are an important addition to recent efforts to solve the conundrum of interpretability of information structures in contexts ranging from machine learning to evolutionary developmental biology [28, 29, 30].

Broader implications

This paper introduces the concept of regulatory nonlinearity as a characteristic of Boolean networks. There are several other related characterizations of Boolean networks such as canalization [31], effective connectivity [11], symmetry [32] and controllability [33]. It has been previously reported that the levels of canalization (a measure of the extent to which fewer inputs influence the outputs of a Boolean function) and the mean effective connectivity (a measure of collective canalization) are high in biological networks [3, 11]. It has also been found that biological networks need few inputs to reprogram [34] and are relatively easier to control [4]. Our formulation of regulatory nonlinearity is related to these other measures in that more linearity implies more apportioning of influence to individual inputs rather than collective sets of inputs (Figure 6). Hence, we hypothesize that regulatory nonlinearity may serve the purpose of controllability and epigenetic stability [35].

Our results further moot the possibility that regulatory nonlinearity may be a factor underlying more powerful dynamical phenomena such as memory [36] and computation, defined as the capacity for adaptive information-processing [37]. Even though there's increasing consensus that biological systems contain memory and perform computation, clarity is lacking as to what features of those systems enable it and what general principles underlie it [37, 38]. Our framework of regulatory nonlinearity offers an approach to answering these questions. For example, one could consider a known dynamical model with a capacity for memory [36] or universal computation such as the elementary cellular automaton (ECA) driven by rule 110 [39] and ask if there are unique properties of its Taylor spectrum that confer their respective capabilities. Present approaches to answering this question typically consists of characterization of the dynamical behavior and not the rules [40, 41, 36]. A characterization of the rules especially makes sense for ECA [42] since the structure is always the same (lattice) and the only feature that distinguishes one ECA from the other is the rule.

Looking at such questions from an even broader perspective it becomes evident that they are only instances of the ultimate puzzle of complex systems, namely what connects the structure and the function of a system. Even though recent work has attempted to answer this question from the perspective of the rules or dynamical laws that govern the system [43, 11, 42], more tools are needed [44]. In that regard, our framework of regulatory nonlinearity could be a novel addition to this burgeoning toolkit in that it could also be applied to continuous differentiable models of biological networks such as those based on differential equations.

Limitations

The main limitation of our formulation of approximability is that the approximation accuracy will necessarily increase with higher orders of approximation since the Taylor terms would be accumulated with each higher order (the highest order of approximation is exact). However, this does not affect the falsifiability of our framework since it's possible, for example, to construct networks with XOR-like functions that would be clearly less linearly approximable than the associated ensembles. The Metastasis model is another example in that regard (Figure 6). Furthermore, though our experiments control for regulatory nonlinearity they don't offer insights into how it dynamically interacts with other network features such as network structure in generating the observed approximability. For example, the network structure may be expected to determine which states the network enters into at any given point that in turn determines which parts of the Taylor compositions are actually utilized and how. Moreover, it's known that certain characteristics of the local regulatory rules, such as "effective connectivity", dynamically modulate the network structure itself [45]. Thus, more research is required to investigate the extent to which the structure and output bias facilitates the high approximability of biological networks and vice versa, for which we already have produced preliminary results by way of the constrained models (Fig 4). Lastly, our conclusions about the linearity of biological regulatory networks may be a reflection of a hidden bias built in the inference methods that produced the models in the first place. We leave it to future work to explore these realms.

2 Data Availability

We used 137 Boolean network models of gene regulation from two sources, namely the *cell collective* [9] and reference [3]. Subsequently, we categorized these models using two types of classifications C1 and C2 as described in Section 1. We provide the details of the classification of each model along with their Pudmed ID and their linear approximation score in the supplementary information file (SI), Table S1.

3 Code Availability

The code that we used for the approximations and the simulations are available through this link: `https://gitlab.com/smanicka/boolion`.

4 Author Contributions

S.M. and D.M. conceived the study; S.M. and K.J. designed code; K.J. performed research and simulations; S.M., K.J., and D.M. analyzed data; M.L. helped bridge the theory to biology. All authors helped in the writing of the manuscript. All authors approved the final version of the manuscript.

5 Acknowledgements

We thank Claus Kadelka for sharing a large repository of Boolean models curated by his group and the accompanying *Python* code for analyzing it. D.M. was partially supported by a Collaboration grant (850896) from the Simons Foundation. M.L. gratefully acknowledges support via grant TWCF0606 of the Templeton World Charity Foundation.

References

[1] Tomasz Kapitaniak and Sajad Jafari. Nonlinear effects in life sciences, 2018.

[2] Michael A Savageau. Design principles for elementary gene circuits: Elements, methods, and examples. *Chaos: An Interdisciplinary Journal of Nonlinear Science*, 11(1):142–159, 2001.

[3] Claus Kadelka, Taras-Michael Butrie, Evan Hilton, Jack Kinseth, and Haris Serdarevic. A meta-analysis of boolean network models reveals design principles of gene regulatory networks. *arXiv preprint arXiv:2009.01216*, 2020.

[4] Enrico Borriello and Bryan C. Daniels. The basis of easy controllability in boolean networks. *Nature Communications*, 12(5227), 2021.

[5] Ruud Stoof and Ángel Goñi-Moreno. Modelling co-translational dimerization for programmable nonlinearity in synthetic biology. *Journal of the Royal Society Interface*, 17(172):20200561, 2020.

[6] Giovanni Pezzulo and Michael Levin. Top-down models in biology: explanation and control of complex living systems above the molecular level. *Journal of The Royal Society Interface*, 13(124):20160555, 2016.

[7] Daniel Lobo, Mauricio Solano, George A Bubenik, and Michael Levin. A linear-encoding model explains the variability of the target morphology in regeneration. *Journal of The Royal Society Interface*, 11(92):20130918, 2014.

[8] Assieh Saadatpour and Réka Albert. A comparative study of qualitative and quantitative dynamic models of biological regulatory networks. *EPJ Nonlinear Biomedical Physics*, 4(1):1–13, 2016.

[9] Tomáš Helikar, B Kowal, and JA Rogers. A cell simulator platform: the cell collective. *Clinical Pharmacology & Therapeutics*, 93(5):393–395, 2013.

[10] Bryan C Daniels, Hyunju Kim, Douglas Moore, Siyu Zhou, Harrison B Smith, Bradley Karas, Stuart A Kauffman, and Sara I Walker. Criticality distinguishes the ensemble of biological regulatory networks. *Physical review letters*, 121(13):138102, 2018.

[11] Santosh Manicka, Manuel Marques-Pita, and Luis M Rocha. Effective connectivity determines the critical dynamics of biochemical networks. *Journal of the Royal Society Interface*, 19(186):20210659, 2022.

[12] George Boole. Collected logical works, vol. i. *Studies in Logic and Probability, R. Rhees (ed.), Open Court Publ. Co., LaSalle, Ill*, 1952.

[13] Ryan O'Donnell. *Analysis of boolean functions*. Cambridge University Press, 2014.

[14] SN Yanushkevich and VP Shmerko. Taylor expansion of logic functions: From conventional to nanoscale design. In *Int. TICSP Workshop on Spectral Methods and Multirate Signal Processing*. Citeseer, 2004.

[15] Melanie Grieb, Andre Burkovski, J Eric Sträng, Johann M Kraus, Alexander Groß, Günther Palm, Michael Kühl, and Hans A Kestler. Predicting variabilities in cardiac gene expression with a boolean network incorporating uncertainty. *PloS one*, 10(7):e0131832, 2015.

[16] Heather Betel and Paola Flocchini. On the relationship between fuzzy and boolean cellular automata. *Theoretical Computer Science*, 412(8-10):703–713, 2011.

[17] Federico Battiston, Enrico Amico, Alain Barrat, Ginestra Bianconi, Guilherme Ferraz de Arruda, Benedetta Franceschiello, Iacopo Iacopini, Sonia Kéfi, Vito Latora, Yamir Moreno, et al. The physics of higher-order interactions in complex systems. *Nature Physics*, 17(10):1093–1098, 2021.

[18] William H Press, Brian P Flannery, Saul A Teukolsky, and William T Vetterling. Numeric recipes in c: the art of scientific computing. *Camb. Univ. Press Camb*, 1992.

[19] Victoria Petri, Pushkala Jayaraman, Marek Tutaj, G Thomas Hayman, Jennifer R Smith, Jeff De Pons, Stanley JF Laulederkind, Timothy F Lowry, Rajni Nigam, Shur-Jen Wang, et al. The pathway ontology–updates and applications. *Journal of biomedical semantics*, 5(1):1–12, 2014.

[20] Mo R Ebrahimkhani and Michael Levin. Synthetic living machines: A new window on life. *Iscience*, page 102505, 2021.

[21] Lina Merchan and Ilya Nemenman. On the sufficiency of pairwise interactions in maximum entropy models of networks. *Journal of Statistical Physics*, 162(5):1294–1308, 2016.

[22] Ryan N Gutenkunst, Joshua J Waterfall, Fergal P Casey, Kevin S Brown, Christopher R Myers, and James P Sethna. Universally sloppy parameter sensitivities in systems biology models. *PLoS computational biology*, 3(10):e189, 2007.

[23] Douglas Hanahan and Robert A Weinberg. Hallmarks of cancer: the next generation. *cell*, 144(5):646–674, 2011.

[24] Minsoo Choi, Jue Shi, Sung Hoon Jung, Xi Chen, and Kwang-Hyun Cho. Attractor landscape analysis reveals feedback loops in the p53 network that control the cellular response to dna damage. *Science signaling*, 5(251):ra83–ra83, 2012.

[25] David PA Cohen, Loredana Martignetti, Sylvie Robine, Emmanuel Barillot, Andrei Zinovyev, and Laurence Calzone. Mathematical modelling of molecular pathways enabling tumour cell invasion and migration. *PLoS computational biology*, 11(11):e1004571, 2015.

[26] Bernard Derrida and Yves Pomeau. Random networks of automata: a simple annealed approximation. *EPL (Europhysics Letters)*, 1(2):45, 1986.

[27] Michael Levin. Bioelectrical approaches to cancer as a problem of the scaling of the cellular self. *Progress in biophysics and molecular biology*, 165:102–113, 2021.

[28] Pantelis Linardatos, Vasilis Papastefanopoulos, and Sotiris Kotsiantis. Explainable ai: A review of machine learning interpretability methods. *Entropy*, 23(1):18, 2020.

[29] Santosh Manicka and Michael Levin. Minimal developmental computation: A causal network approach to understand morphogenetic pattern formation. *Entropy*, 24(1):107, 2022.

[30] Richard A Watson, Michael Levin, and Christopher L Buckley. Design for an individual: connectionist approaches to the evolutionary transitions in individuality. *Frontiers in Ecology and Evolution*, page 64, 2022.

[31] Stuart Kauffman. The large scale structure and dynamics of gene control circuits: an ensemble approach. *Journal of Theoretical Biology*, 44(1):167–190, 1974.

[32] CJ Olson Reichhardt and Kevin E Bassler. Canalization and symmetry in boolean models for genetic regulatory networks. *Journal of Physics A: Mathematical and Theoretical*, 40(16):4339, 2007.

[33] Alexander J Gates and Luis M Rocha. Control of complex networks requires both structure and dynamics. *Scientific reports*, 6(1):1–11, 2016.

[34] Franz-Josef Müller and Andreas Schuppert. Few inputs can reprogram biological networks. *Nature*, 478(7369):E4–E4, 2011.

[35] Andreas Wagner. Does evolutionary plasticity evolve? *Evolution*, 50(3):1008–1023, 1996.

[36] Surama Biswas, Santosh Manicka, Erik Hoel, and Michael Levin. Gene regulatory networks exhibit several kinds of memory: Quantification of memory in biological and random transcriptional networks. *Iscience*, 24(3):102131, 2021.

[37] Melanie Mitchell. Ubiquity symposium: biological computation. *Ubiquity*, 2011(February), 2011.

[38] Dominique Chu, Mikhail Prokopenko, and J Christian J Ray. Computation by natural systems, 2018.

[39] Matthew Cook et al. Universality in elementary cellular automata. *Complex systems*, 15(1):1–40, 2004.

[40] Stephen Wolfram. Statistical mechanics of cellular automata. *Reviews of modern physics*, 55(3):601, 1983.

[41] Hector Zenil and Jürgen Riedel. Asymptotic intrinsic universality and natural reprogrammability by behavioural emulation. In *Advances in Unconventional Computing*, pages 205–220. Springer, 2017.

[42] Santosh Venkatiah Sudharshan Manicka. *The role of canalization in the spreading of perturbations in Boolean networks*. PhD thesis, Indiana University, 2017.

[43] Manuel Marques-Pita and Luis M Rocha. Canalization and control in automata networks: body segmentation in drosophila melanogaster. *PloS one*, 8(3):e55946, 2013.

[44] Luis M Rocha. On the feasibility of dynamical analysis of network models of biochemical regulation. *arXiv preprint arXiv:2110.10821*, 2021.

[45] Alexander J Gates, Rion Brattig Correia, Xuan Wang, and Luis M Rocha. The effective graph reveals redundancy, canalization, and control pathways in biochemical regulation and signaling. *Proceedings of the National Academy of Sciences*, 118(12):e2022598118, 2021.

Supplementary Information

The nonlinearity of regulation in biological networks

Santosh Manicka, Kathleen Johnson, Michael Levin and David Murrugarra

1. Probabilistic generalization of Boolean logic

Here we show that $\hat{f}$ is a generalization of f in the sense that $\hat{f}(x) = f(x)$ for all $x \in \{0,1\}^n$.

Theorem 0.1. *For discrete values of $x_i \in \{0,1\}$, $i = 1, \ldots, n$, we have*

$$\hat{f}(x_1, \ldots, x_n) = f(x_1, \ldots, x_n).$$

Proof. Let $z = (z_1, \ldots, z_n) \in \{0,1\}^n$. Since each z_i is either 0 or 1, we have that $p_i = 1$ if $z_i = 1$ or $p_i = 0$ if $z_i = 0$ for $i = 1, \ldots, n$. We want to show that $\hat{f}(p_1, \ldots, p_n) = f(z_1, \ldots, z_n)$. Since $X = R_0^f \cup R_1^f$, we have that either $z \in R_0^f$ or $z \in R_1^f$. If $z \in R_1^f$, then $f(z) = 1$ and $Pr(z) = \prod_{i=1}^n \hat{p}_i = 1$. Moreover, for any other $x \in R_1^f$ with $x \neq z$ we have that $Pr(x) = 0$. Thus, $\hat{f}(z) = \sum_{x \in R_1^f} Pr(x) = Pr(z) = 1$. Now if $z \in R_0^f$, then $\hat{f}(z) = 0$ because $\sum_\emptyset = 0$. Thus, $\hat{f}(x) = f(x)$ for all $x \in \{0,1\}^n$. □

2. Maximum absolute value of a Taylor derivative

Here we show that $\max(|\partial^\alpha \hat{f}|) = (\min(p, 0.5) - \max(p - 0.5, 0))2^{|\alpha|}$.
We begin with the definition of the derivative given by

$$\frac{\partial \hat{f}(x_1, \ldots, x_i, \ldots, x_k)}{\partial x_i} = \lim_{h \to 0} \frac{\hat{f}(0.5, \ldots, h, \ldots, 0.5) - \hat{f}(0.5, \ldots, 0, \ldots, 0.5)}{h}$$

Since $\hat{f}$ is a pseudo-Boolean function and hence a multilinear polynomial [1], we can rewrite it by setting h to 1, as a finite difference; the idea being that the derivative taken over any point on a line is the line itself:

$$\frac{\partial \hat{f}(x_1, \ldots, x_i, \ldots, x_k)}{\partial x_i} = \hat{f}(0.5, \ldots, 1, \ldots, 0.5) - \hat{f}(0.5, \ldots, 0, \ldots, 0.5)$$

Since multilinear interpolation can be formulated as weighted averaging [2], we can further rewrite it as follows (the weights are equal here since the non-binary values are all set to 0.5):

$$\frac{\partial \hat{f}(x_1, \ldots, x_i, \ldots, x_k)}{\partial x_i} = \sum_{x_1, \ldots, x_{i-1}, x_{i+1}, \ldots, x_k \in \{0,1\}} \frac{\hat{f}(x_1, \ldots, x_{i-1}, 1, x_{i+1}, \ldots, x_k) - \hat{f}(x_1, \ldots, x_{i-1}, 0, x_{i+1}, \ldots, x_k)}{2^{k-1}}$$

As can be seen, there are a total of 2^k terms, with half of them positively signed and half negative. This form of expression generalizes to derivatives taken over two or more variables. For example, the derivative taken over two variables, x_i and x_j, looks as follows:

$$\frac{\partial^2 \hat{f}(\ldots, x_i, \ldots, x_j, \ldots)}{\partial x_i \partial x_j} = \sum_{x_1, \ldots, x_{i-1}, x_{i+1}, \ldots, x_k \in \{0,1\}} \sum_{x_1, \ldots, x_{j-1}, x_{j+1}, \ldots, x_k \in \{0,1\}} \left[\frac{\hat{f}(\ldots, x_{i-1}, 1, x_{i+1}, \ldots, x_{j-1}, 1, x_{j+1}, \ldots) - \hat{f}(\ldots, x_{i-1}, 1, x_{i+1}, \ldots, x_{j-1}, 0, x_{j+1}, \ldots)}{2^{k-2}} \right] - \left[\frac{\hat{f}(\ldots, x_{i-1}, 0, x_{i+1}, \ldots, x_{j-1}, 1, x_{j+1}, \ldots) - \hat{f}(\ldots, x_{i-1}, 0, x_{i+1}, \ldots, x_{j-1}, 0, x_{j+1}, \ldots)}{2^{k-2}} \right]$$

Following rearrangement of terms it becomes evident that this expression also contains 2^{k-1} positive terms and 2^{k-1} negative terms, with the only difference in the power of the denominator term. It can thus be concluded that any derivative $\partial^\alpha \hat{f}$ (in multi-index notation) has 2^{k-1} positive terms and 2^{k-1} negative terms.

A straightforward way to maximize the value of a derivative expressed in this form is by assigning as many instances of 1 as possible to the positive terms and as few instances of 1 as possible to the negative terms. For a Boolean function with k inputs and output bias p, this can be accomplished by assigning $\min(2^{k-1}, p2^k)$ ones and $\max(p2^k - 2^{k-1}, 0)$ ones respectively. Therefore,

$$\begin{aligned}\max(|\partial^\alpha \hat{f}|) &= \frac{\min(2^{k-1}, p2^k) - \max(p2^k - 2^{k-1}, 0)}{2^{k-|\alpha|}} \\ &= (\min(p, 0.5) - \max(p - 0.5, 0))2^{|\alpha|}; 1 \leq |\alpha| \leq k.\end{aligned}$$

Note that this formula only applies to a specific order of nonlinearity $|\alpha|$ independent of the other orders within the same Boolean function. In actuality, there are dependencies between the various orders within a Boolean function. That is, if a Boolean function were to be constructed such that the derivative of a particular order $|\alpha_1|$ is maximized then there's no guarantee that the derivative of another order $|\alpha_2| \neq |\alpha_1|$ could be simultaneously maximized. This is one of the limitations of the normalization for which the above formula is used.

Table 1: Dataset Description

Pubmed ID	**Description**	**Category 1**	**Category 2**	**Linear Approximability**
18852469	A model describing the survival of cytotoxic T lymphocytes in Tcell large granular lymphocyte (T-LGL) leukemia	Disease	Metazoan	80.28235
22102804	A model of Tcell large granular lymphocyte (T-LGL) leukemia	Disease	Cancer	79.27166
26102287	A model describing the infection response of Clostridium difficile to antibiotic treatment	Disease	Primitive	75.69523
23169817	A model of the simplified p53 network with low DNA damage	Disease	Cancer	72.36818
24564942	A threshold model of the C. elegans early embryonic cell-cycle	Regulatory	Metazoan	62.13963
23169817	A model of the simplified p53 network with high DNA damage	Disease	Cancer	59.89628
28209158	A model of tumorigenic transformation of human epithelial cells	Disease	Cancer	57.49518
30104572	A model of cell state transition of epithelial-to-mesenchymal transition (EMT)	Disease	Cancer	56.90066
25189528	A model of epithelial-to-mesenchymal transition (EMT) integrating the signaling pathways involved in developmental EMT and known dysregulations in invasive hepatocellular carcinoma (HCC)	Disease	Metazoan	56.86491
29632237	A model used to identify key protiens regulating bortezomib	Disease	Cancer	55.24462

31516637	A model of cellularmetabolic flexibility where The inhibitor, Pyruvate, only blocks PDKactivity when at least one of its activators is absent from the system.	Metabolic	Metazoan	54.61028
19185585	A model of budding yeast cell-cycle	Regulatory	Primitive	54.46379
27148350	A model linking the nerve growth factor NGF to the proliferation or differentiation outcomes of the cell	Biochemical	Metazoan	52.98308
23081726	A model of the Influenza A virus replication cycle	Disease	Primitive	52.82458
26573569	A regulatory network model of the differentiation of the human gonadal cells into testes or ovaries	Regulatory	Metazoan	52.75945
31516637	A model of cellularmetabolic flexibility where the inhibitor, Pyruvate, always blocks PDKactivity when it is present in the system.	Metabolic	Metazoan	52.21167
30038409	A model of genes/proteins responsible for loss/gain offunction in human pluripotent stem cells	Regulatory	Metazoan	51.17677
24970389	A protein interaction model to elucidate drug resistance in breast cancer	Disease	Cancer	50.66349
22102804	A reduced model of Tcell large granular lymphocyte (T-LGL) leukemia	Disease	Metazoan	50.23742
31130988	FA-CHKREC (G2 checkpoint and the checkpoint recovery) model, which explores how FA cells might use DDA (DNA damage adaptation)	Disease	Metazoan	45.55726
32054948	A model of the G1/S checkpoint regulation contemplating the regulatory influences of both miR-34a and miR-16	Disease	Metazoan	45.41591
16542429	A model of the regulatory network governing the differentiation of CD4+ T cells	Biochemical	Metazoan	44.35813
26244885	A model of the Septation Initiation Network that controls cytokinesis in fission yeast	Regulatory	Metazoan	44.00536
22253585	A model of host immune response to single and coinfection	Disease	Primitive	43.39992
30024932	A model of the G2/M checkpoint arrest regulation contemplating the influence of miR-449a	Disease	Metazoan	41.20924
29378814	a model to predict stabilized Pluripotent stem cells (PSC)gene regulatory network (GRN) states in response to input signals	Regulatory	Metazoan	39.44636
28584084	A model encompassing the main transcription factors and signaling components involved in myeloid and lymphoid development.	Biochemical	Metazoan	38.83446

24970389	A protein interaction model to elucidate drug resistance in breast cancer	Disease	Cancer	38.59772
19524598	The simplified model of regulation of apoptosis via the NFkB pathway	Biochemical	Metazoan	37.31991
22448278	A model of Mycobacterium tuberculosis	Disease	Primitive	35.75686
24970389	A cell signaling network model to elucidate drug resistance in breast cancer	Disease	Cancer	34.81927
30953496	A model integrating the insulin resistance pathway with pancreatic Œ-cell apoptosis pathway which are responsible for Type 2 diabetes mellitus (T2DM)	Disease	Metazoan	34.81698
24970389	A protein interaction model to elucidate drug resistance in breast cancer	Disease	Cancer	34.08386
31949240	A model of renovascular disease (RVD)	Disease	Metazoan	33.98901
28426669	A model of the gene regulatory network Arabidopsis thaliana	Regulatory	Plants	33.95125
28639170	A model of the wellknown arabinose operon in E. coli	Metabolic	Primitive	33.72184
21853041	A model of myeloid differentiation	Regulatory	Metazoan	32.63689
30953496	A model integrating the insulin resistance pathway with pancreatic Œ-cell apoptosis pathway which are responsible for Type 2 diabetes mellitus (T2DM)	Disease	Metazoan	32.06319
28381275	A model of colorectal tumorigenesis	Disease	Cancer	32.06171
26616283	A model of oncogenic pathways in NB	Disease	Cancer	31.66786
26340681	A model of cell-cycle regulation in plants	Regulatory	Plants	31.66438
23868318	A model of FGF signaling pathway in drosophila	Regulatory	Metazoan	31.52491
25908096	A model of iron acquisition and oxidative stress response in the fungal pathogen aspergillus fumigatus	Metabolic	Primitive	31.51053
22267503	A model of Fanconi Anemia/Breast Cancer pathway elucidating the repair of DNA strands	Disease	Metazoan	31.23094
26244885	A model of the Septation Initiation Network	Regulatory	Metazoan	31.0255
27542373	A model of the allowed long-term behaviors of the stomatal opening process in plants	Signaling	Plants	30.77432
28426669	A model of the gene regulatory network Arabidopsis thaliana	Regulatory	Plants	30.44945
24970389	A protein interaction model to elucidate drug resistance in breast cancer	Disease	Cancer	30.28947
31516637	A model of cellular metabolic flexibility where Fatty Acid mediated activation of PDK bypasses Pyruvate mediated inhibition.	Metabolic	Metazoan	29.3459

29237040	A logical model of initiation of the metastatic process in cancer	Disease	Cancer	28.56148
16464248	A model of the Tcell receptor signaling	Signaling	Metazoan	27.97508
24970389	A protein interaction model to elucidate drug resistance in breast cancer	Disease	Cancer	27.57258
22253585	A model of host immune response to single and coinfection	Disease	Primitive	27.4484
22192526	A model of the Arabidopsis thaliana root stemcell niche	Signaling	Plants	27.19403
29230182	A model of the molecular regulatory network involved in the control of angiogenesis	Biochemical	Metazoan	26.51007
30116195	A model of the regulation in the differentiation process of major Tcell subtypes, i.e., Th1, Th2, Th17 and iTreg cells.	Biochemical	Metazoan	26.25546
23743337	A gene regulatory network model of T lymphocyte differentiation	Regulatory	Metazoan	26.18992
24079299	A regulatory model of Salmonella typhimurium	Disease	Primitive	25.50749
28187161	A Boolean network CARENET (CAmbium REgulation gene NETwork) for modeling cambium activity	Regulatory	Plants	24.49806
26207376	A model of gene regulation in the cardiac progenitor cells involved in early vertebrate development	Regulatory	Metazoan	23.17666
27464342	A model of the M1 (LPS-activated) and M2 (IL-4/13-activated) macrophage polarization types	Signaling	Metazoan	22.47601
11082279	A model of the ras,Äìraf,ÄìMAPK/ERK signaling pathway	Biochemical	Metazoan	22.18949
24250280	A comprehensive and generic reaction map for the MAPK signaling network	Disease	Metazoan	21.58656
29622038	A phenotype control kernel (PCK) model of the mitogen-activated protein kinase(MAPK) model	Disease	Metazoan	21.54371
26385365	A model of how mutations in the FA/BRCA pathway cause Fanconi anemia	Disease	Metazoan	21.48794
22253585	A model of within-host immunodynamics	Disease	Primitive	20.64292
26408858	A model of the regulatory network of lymphopoiesis	Regulatory	Metazoan	20.25874
24376455	A model of a metastatic melanoma network	Disease	Cancer	20.25273
24069138	A threshold model of the cell-cycle control network of yeast S. pombe	Regulatory	Primitive	20.16704
26751566	A dynamic model for the regulatory network that controls terminal B cell differentiation	Biochemical	Metazoan	19.476

25538703	A model elucidating the role of the CAV1 scaffold protein in Tcell leukemia	Disease	Metazoan	19.43595
31516637	A model of cellularmetabolic flexibility where Acetyl-CoA mediated activation of PDK bypasses Pyruvate mediated inhibition.	Metabolic	Metazoan	19.41784
29186334	A model to describe temporal expression patterns observed in GMP-derived cells	Regulatory	Metazoan	18.79806
1753781	A model of tumor immunity	Disease	Cancer	18.37732
23868318	A model of receptor signaling pathways, including EGFR, G-protein-coupled receptor, integrin, and stress pathways	Regulatory	Metazoan	16.81161
17722974	A model of Tcell activation via the Tcell receptor, the CD4/CD8 co-receptors, and the accessory signaling receptor CD28	Signaling	Metazoan	16.73999
30281473	A model of the aberrant signaling in pancreatic cancer	Disease	Cancer	16.02394
20169167	A model of the Pseudomonas syringae	Disease	Primitive	15.87294
23056457	A model of gene regulation underlying early cardiac development in mammals	Regulatory	Metazoan	15.83555
28361666	A model of castration-resistant prostate cancer	Disease	Cancer	15.29735
27138333	A model of the signaling network associated with RCP-driven invasive migration	Disease	Cancer	15.04079
16968132	A model of water conservation via stomatal opening in plants	Signaling	Plants	13.58676
20221256	A model of the interplay between the NFkB pro-survival pathway, RIP1-dependent necrosis, and the apoptosis pathway in response to death receptor-mediated signals	Biochemical	Metazoan	13.55924
23233838	A signaling pathway model of apoptosis in yeast	Regulatory	Primitive	12.98085
29596489	A mathematical in silico model that robustly recapitulates the crosstalk between IGF and Wnt signaling.	Signaling	Metazoan	12.92163
22962472	A model of keratinocyte cell migration mediated by hepatocyte growth factors	Signaling	Metazoan	12.1657
27613445	A model of the signaling pathways that control S-phase entry and a specific-type of senescence called geroconversion	Regulatory	Metazoan	10.90313
18463633	A model of cyclic gene expression during cell division in budding yeast	Regulatory	Primitive	10.87729
25063553	A model of the hormonal control of hepatic metabolism using insulin and glucagon signaling	Metabolic	Metazoan	10.86576

25063553	A model of the hormonal control of hepatic metabolism using insulin and glucagon signaling	Metabolic	Metazoan	9.87147
23868318	A model of receptor signaling pathways, including EGFR, G-protein-coupled receptor, integrin, and stress pathways	Regulatory	Metazoan	9.859414
20221256	A model of apoptosis involving death-receptor mediated signals	Regulatory	Metazoan	9.835997
25163068	A model of the complete quorum sensing system of Pseudomonas aeruginosa	Signaling	Primitive	9.655856
19422837	A model of apoptosis involving external growth factors	Signaling	Metazoan	9.007914
16873462	A model of the mammalian cell-cycle	Regulatory	Metazoan	8.110625
30518777	A model of the ABA signaling pathway	Signaling	Plants	7.068097
25780058	A model of a Rho-family GTPases signaling network	Disease	Metazoan	6.516515
25063553	A model of the hormonal control of hepatic metabolism using insulin and glucagon signaling	Metabolic	Metazoan	6.489934
25063553	A model of the hormonal control of hepatic metabolism using insulin and glucagon signaling	Metabolic	Metazoan	6.431252
26163548	A signaling pathway model describing the interaction between a drug and cellular outcomes in multiple myeloma cells	Signaling	Metazoan	5.942066
29206223	A model to predict different in-silico knockouts that prevent key SASP-mediators, IL-6 and IL-8, from getting activated upon DNA damage	Biochemical	Metazoan	5.414375
26446703	A model of colitis-associated colon cancer involving P53, MDM2, and AKT	Disease	Metazoan	4.918872
19144179	A model of glucose regulation in yeast	Metabolic	Primitive	4.804903
30530226	A model of the crosstalk between the TGF-Œ,p38 MAPK and cell-cycle checkpoint pathways which qualitatively describes this dual behavior of TGF-Œ	Signaling	Metazoan	4.597779
21563979	A model of glucose regulation via the Lac operon	Metabolic	Primitive	3.447058
23049686	A model of cell-cycle in budding yeast	Regulatory	Primitive	3.288717
23868318	A model of receptor signaling pathways, including EGFR, G-protein-coupled receptor, integrin, and stress pathways	Regulatory	Metazoan	2.027278
17010384	A model used to simulate a molecular pathway between two neurotransmitter receptors: dopamine and glutamate receptors	Signaling	Metazoan	0.686516

23171249	A regulatory model of the TOL multi-protein complex system found on the cell membrane of gram negative bacteria	Metabolic	Metazoan	0.508221
23868318	A model of interaction between nine key signaling pathways in drosophila	Regulatory	Metazoan	0.074953
16464248	A model of a typical signaling pathway where mass and signal flow occur simultaneosly	Signaling	Metazoan	0
18194572	A logical model of HGF and H. pylori induced c-Met signal transduction	Disease	Metazoan	0
27594840	A model linking the hematopoietic stem progenitor cells and mesenchymal stromal cells in the bone marrow	Disease	Metazoan	-0.19119
23520449	A model of body segmentation in drosophila melanogaster	Biochemical	Metazoan	-0.30788
23764028	A model of the effect of TGF-b1 on misquitos with the parasite Plasmodium falciparum	Disease	Metazoan	-0.71147
21639591	A model for phospholipase C-coupled calcium signaling pathways	Signaling	Metazoan	-0.76057
18433497	A model of cellular immune response integrating toll-like receptor, interferon, NF-kappaB and apoptotic pathways	Signaling	Metazoan	-1.00938
19025648	A model of physiological regulation in cholestrol biosynthesis	Metabolic	Metazoan	-1.24445
30546316	A model for the generegulation driving macrophage polarization to the M1, M2a, M2b, and M2c phenotypes	Signaling	Metazoan	-2.01878
23469179	A model of cancer network regulated by miR-17-92 cluster	Disease	Cancer	-2.71715
19118495	A regulatory model of the cell-cycle involving the transmembrane tyrosine kinase ERBB2	Disease	Metazoan	-3.46556
23134720	A model linking the oxidative stress pathway to apoptosis	Biochemical	Metazoan	-3.86379
26346668	A model is used to map environmental and flow induced signals to endothelial cell phenotype (proliferation,migration, apoptosis, and lumen formation)	Disease	Cancer	-4.09752
32870080	A model of the lac operon with feedback	Regulatory	Primitive	-4.53977
26090929	An integrated regulatory and signaling pathway model of the fate of the CD4+ T immune cells	Biochemical	Metazoan	-6.53616
20659480	ABA-induced closure model (ABA signal transduction network)	Signaling	Plants	-9.87253
25980672	A model of the melanogenesis signaling network	Signaling	Metazoan	-9.90163

21968890	A model of signaling pathway involving the pro-inflammatory cytokines interleukin 1 (IL-1)	Signaling	Metazoan	-13.6196
31048917	A model of Drosophila melanogaster	Regulatory	Metazoan	-13.6436
23868318	A model of interaction between nine key signaling pathways in drosophila	Regulatory	Metazoan	-13.9899
21968890	A model of signaling pathway involving the pro-inflammatory cytokines interleukin 6 (IL-6)	Signaling	Metazoan	-14.0946
19622164	A model of the external signaling molecule TNFa	Disease	Metazoan	-17.2082
19622164	A model of the external signaling molecule TNFb1	Disease	Metazoan	-17.4249
28455685	A model of the epidermal growth factor receptor signaling of a breast epithelial cell line, MFC10A.	Disease	Cancer	-18.4117
30323768	A model gene regulatory network (GRN) of latent proviruses in resting CD4+ Tcell to visualize thecomplexity of the HIV-1 gene expression	Disease	Metazoan	-20.8165
26528548	A regulatory network model of early metasis development	Disease	Cancer	-78.6659
20862356	A gene regulatory model of spatial expression patterns in the cerebral cortex	Regulatory	Metazoan	-92.6647

References

[1] Peter L Hammer, I Rosenberg, Sergiu Rudeanu, et al. On the determination of the minima of pseudo-boolean functions. *Studii si Cercetari matematice*, 14:359–364, 1963.

[2] William H Press, Brian P Flannery, Saul A Teukolsky, and William T Vetterling. Numeric recipes in c: the art of scientific computing. *Camb. Univ. Press Camb*, 1992.